PAPER

NJC
www.rsc.org/njc

# $W(CO)_5$-pyridine π-acceptor complexes: theoretical calculations and a laser photolysis study

**Janusz Zakrzewski,*[a] Jacques A. Delaire,[b] Chantal Daniel[c] and Isabelle Cote-Bruand[c]**

[a] *Department of Organic Chemistry, University of Łódź, Narutowicza 68, 90-136 Łódź, Poland. E-mail: janzak@uni.lodz.pl; Fax: (+42) 678 65 83; Tel: (+42) 678 47 50*
[b] *Laboratoire de Photophysique et Photochimie Supramoléculaires et Macromoléculaires (CNRS UMR 8531), Ecole Normale Supérieure de Cachan, 94235 Cachan cédex, France. E-mail: jdelaire@ppsm.ens-cachan.fr; Fax: (+33) 1 47 40 24 54; Tel: (+33) 1 47 40 53 37*
[c] *Laboratoire de Chimie Quantique (CNRS UMR 7551), Université Louis Pasteur, Institut Le Bel, 4, rue Blaise Pascal, 67000 Strasbourg, France. E-mail: daniel@quantix.u-strasbg.fr; Fax: (+33) 3 90 24 15 89; Tel: (+33) 3 90 24 13 02*

***Received (in Toulouse, France) 7th June 2004, Accepted 3rd September 2004***
***First published as an Advance Article on the web 15th November 2004***



Theoretical (time-dependent DFT and MS-CASPT2) calculations showed that the two lowest-energy excited states of $W(CO)_5$ complexes of 4-[(*E*)-2-carbomethoxy-2-cyanovinyl)]pyridine, **1** and 4-(2,2-dicyanovinyl)pyridine, **2** have metal-to-ligand charge transfer (MLCT) character. They result from an electron transfer from a tungsten-centered orbital ($5d_{x^2-y^2}$ or $5d_{xy}$) to the π* orbital localized on the ethylenic bridge. The calculated lowest excitation energy for **1** (537 nm) is close to the experimental value of 522 nm in cyclohexane. Laser flash photolysis at 532 nm in the nanosecond and picosecond domains showed that for both complexes transient excited states are formed with a quantum yield close to 1. Their lifetimes are about 10 times shorter than those observed previously for similar $W(CO)_5$-pyridine complexes, with the lifetime of the excited state of compound **1** being longer than that of compound **2**. Increasing the solvent polarity decreases the lifetimes in both cases. Complexes **1** and **2** are nonfluorescent, photostable, and do not undergo photosolvation.

## Introduction

Photochemistry and photophysics of complexes $W(CO)_5$–L, where L is a pyridine-type nitrogen ligand, have been thoroughly studied.[1–8] It is generally admitted that electronic excitation of such complexes leads to ligand field (LF or d-d) or metal-to-ligand charge transfer (MLCT) excited states. The latter becomes the lowest excited state when the pyridine ligand bears in position 4 electron-withdrawing substituents such as acyl or cyano groups. The LF states are believed to be involved in photochemical ligand substitution reactions, which explains the fact that compounds for which an MLCT state is the lowest excited state undergo photosubstitution with much lower quantum yields than compounds having the lowest LF state.[1] It is also worth noting that a recent computational study on $W(CO)_5$–pyridine and $W(CO)_5$–4-cyanopyridine complexes suggest that LF states are much higher in energy than M → CO* charge transfer (CT) transitions and are not accessible by irradiation in the visible region.[9] Therefore, the absorption bands earlier assigned to LF transitions (~400–410 nm) may correspond to the MLCT transitions. In the case of the complex with the unsubstituted pyridine, the M → CO* CT state is the lowest one and the M → pyridine* CT state is higher in energy whereas the opposite is observed in the 4-cyanopyridine complex.

Complexes in which the M → pyridine* CT state is the lowest excited state luminesce in fluid solutions[1,3] with relatively long lifetimes (in the hundreds of ns) and exhibit enhanced second-order nonlinear optical properties.[10]

Recently, we described the synthesis of $W(CO)_5$ complexes of 4-[(*E*)-2-carbomethoxy-2-cyanovinyl)]pyridine, **1**, and 4-(2,2-dicyanovinyl)pyridine, **2** (Chart 1).[11] Because of the strong electron-accepting properties of the pyridine ligands in these complexes, their electronic absorption spectra show extremely low-energy charge transfer bands, which are well separated from higher energy (LF or M → CO*) bands. It seemed to us interesting to see if the character of the electronic transitions could be predicted by computational methods used earlier for complexes having weaker acceptor groups in the pyridine ligands.[9] On the other hand, we wanted to get insight into the dynamic properties of the lowest excited states in these compounds by using time-resolved laser flash spectroscopy. Herein we report the results of this study.

## Experimental

Compounds **1** and **2** were prepared and purified according to earlier published procedures.[11]

### Computational details

The geometries of complexes **1** and **2** have been optimized at the DFT level of theory using the B3LYP functional within the relativistic effective core potentials (ECP), in the small core approximation, and with the following valence basis sets: for the tungsten center ($Z = 14$), a (8s,7p,6d) set contracted to [6s,5p,3d];[12] for the carbon atoms ($Z = 4$) and nitrogen atoms ($Z = 5$), a (4s,4p) set contracted to [2s,2p]; for the oxygen atoms ($Z = 6$), a (4s,5p) set contracted to [2s, 3p];[13] and for the hydrogen atoms, a (4s) set contracted to [2s].[14] The geometry optimizations have been performed under the $C_s$ symmetry constraint. This is justified by the convergence of the initial $C_1$ structure of **2** to a $C_s$ equilibrium geometry in the gas phase.[15] The subsequent calculations of excited states at different levels

DOI: 10.1039/b408617a

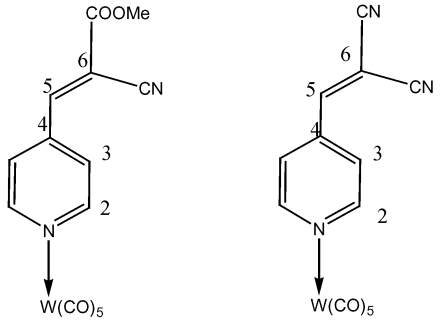


**Chart 1** Compounds **1** and **2**. Labelling of carbon atoms in the pyridine ligands is arbitrary and is introduced only for clarity in the discussion of the theoretical calculation results.

of theory (time-dependent DFT,[16] complete active space SCF/multistate CASPT2[17,18]) have been performed with the same basis sets using the $C_s$ DFT optimized geometries.

The transition energies to the low-lying excited states of complexes **1** and **2** (near the UV/Visible domain of energy) have been calculated by means of the time-dependent DFT (TD-DFT) approach. In order to validate the TD-DFT results for this class of molecules the absorption spectrum of **1** has been studied at the CASSCF level based on 10 electrons correlated in 12 orbitals (the $5d_W$ occupied orbitals and the corresponding $5d'_W$, the $\pi_{CC}$ and $\pi^*_{CC}$ orbitals localized on the pyridine ligand and four $\pi^*_{CO}$). The CASSCF calculations have been averaged over 10 roots for each symmetry (A′ and A″). The remaining dynamical correlation effects on the transition energies have been obtained by means of the MS-CASPT2 approach. The calculations have been performed either with GAUSSIAN[19] (DFT, TD-DFT) or MOLCAS 5.0[20] quantum chemistry software.

### Laser photolysis

Transient absorption spectroscopy was carried out with nanosecond and picosecond Nd-YAG lasers. Both setups have been described previously.[21,22] The mode-locked picosecond Nd:YAG laser was manufactured by BM Industries (model BMI 502 DPS). The pulse generation consisted in an oscillator, an actively-passively mode-locked cavity, an extra-cavity Pockels cell located between crossed polarizers and two single-pass Nd:YAG amplifiers. At the output of the second amplifier, the energy was about 30 mJ in a single pulse (35 ps pulse width, 8 Hz) at 1064 nm. After passing through one harmonics-generating KDP crystal, the beam was composed of two wavelengths (1064 nm and 532 nm) that were split into two separated beams by appropriate dichroic mirrors. The second harmonics (532 nm) beam was used as the pump beam and the fundamental beam (1064 nm) was used to generate a probe beam in the following way: using a procedure described by Sumitani and Yoshihara,[23] the fundamental flash of the laser was focused on a tungsten electrode in a glass cell filled with xenon at a pressure of 2 bars. The laser created a plasma whose emission lifetime was *ca.* 50 ns with a rise time (<100 ps) during the pulse width and an emission plateau after a 10 ns delay. This light source did not need any electronic setup and had a continuous emission spectrum between 300 and 800 nm with a maximum near 400 nm, that is, very similar to the emission of a xenon arc. Both probe and pump beams were focused by separate lenses on the middle of a cell (1 mm optical path) in a nearly colinear arrangement, with an angle of 20°. The probe beam volume was contained inside the larger excitation beam volume. At the output of the cell, the pump beam was blocked with an iris and the probe beam was focused on the entrance slit of a monochromator. The output signal at a selected wavelength was detected by a streak camera (ARP) with a time resolution of 8 ps. The solution was circulated through the cell in order to prevent multiple flashing on the same volume, which must be avoided in photochromic systems.

The nanosecond laser was a Q-switched Nd:YAG laser manufactured by BM Industries (model BMI 502 DNS 77/10), delivering 7 ns pulses at 1064 nm. The output energy was 120 mJ at 532 nm. The excitation beam and the probe beam generated by a pulsed xenon source were perpendicular to each other inside the 1 cm × 1 cm cell. The analyzing beam was spectrally dispersed by a monochromator and converted into an electric signal by a Hamamatsu R928 PM tube. The electric signal was recorded by a digital-memory oscilloscope (Tektronix TDS 654C) connected to a PC. The transient signals were analyzed by a custom routine using the Igor procedure (Igor Pro Version 4, Wavemetrics Inc.). Each given rate constant is the mean value of at least five different measurements.

Due to perturbation by the excitation wavelength (532 nm), transient absorption measurements in a wavelength range comprised between 500 and 550 nm was not possible.

## Results

### Theoretical calculations of the ground state geometries

The calculated DFT (B3LYP) equilibrium geometries of the ground state of complexes **1** and **2** are depicted in Fig. 1 together with the observed geometries in the crystalline state. The optimized structures are compared to those determined by X-ray diffraction.[11] Both molecules show energy minima corresponding to the $C_s$ conformations in which the pyridine plane bisects the $C_{eq}$–W–$C_{eq}$ bond angle. Some optimized relevant distances and bond angles are reported in Table 1 and compared with those determined by X-ray diffraction.

There is a good agreement between calculated and observed bond lengths and angles with the exception of the $(CO)_{ax}$WN and $NC_4C_5C_6$ bond angles, which do not reflect the distortion of the pyridine ligand observed in the X-ray structures as shown in Fig. 1. These distortions are undoubtedly due to crystal packing effects since an energy optimization starting from the X-ray geometries leads also to the planar structures.

### Theoretical calculations of the low energy electronic transitions

The TD-DFT and CASSCF/MS-CASPT2 calculations of the electronic transitions to the low-lying excited states of complexes **1** and **2** were based on the DFT optimized geometries. The electronic configuration of the electronic ground states of **1** and **2,** both having a $d^6$ W(0) central atom, can be described as follows: $(\pi_{C=C})^2(d_{x^2-y^2})^2\ (d_{xz})^2(d_{yz})^2(\pi_{C=C})^0(\pi_{CO})^0$. Similarly as for complexes of pyridine and 4-cyanopyridine, the empty orbitals $d_{xy}$ and $d_z^2$ in **1** and **2** are too high in energy to be populated by an excitation in the visible region (Fig. 2).

According to the qualitative molecular orbital diagram deduced from the CASSCF calculation of the electronic

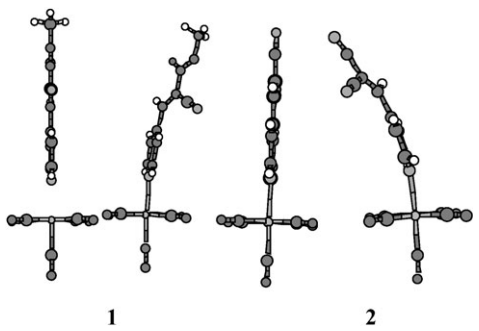


**Fig. 1** DFT optimized $C_s$ geometries (leftmost structure of each pair) and X-ray structures (rightmost structure of each pair) of complexes **1** and **2**.

**Table 1** DFT (B3LYP) optimized bond lengths (in Å) and bond angles (in °) of compounds **1** and **2** compared to X-ray diffraction structural data.[11]

| | **1** | | **2** | |
|---|---|---|---|---|
| | Calculated | X-ray | Calculated | X-ray |
| W–N | 2.30 | 2.27 | 2.30 | 2.27 |
| $W–CO_{eq}$ | 2.06 | 2.07 (2.07) | 2.06 | 2.07 (2.03) |
| $W–CO_{eq}$ | 2.06 | 2.03 (2.04) | 2.06 | 2.07 (2.00) |
| $W–CO_{ax}$ | 2.01 | 1.98 | 2.01 | 1.99 |
| $C_4–C_5$ | 1.46 | 1.46 | 1.46 | 1.46 |
| $C_5–C_6$ | 1.36 | 1.33 | 1.34 | 1.31 |
| $C_6–CN$ | 1.42 | 1.43 | 1.43 | 1.42 |
| $C_6–CN(COOCH_3)$ | 1.49 | 1.50 | 1.43 | 1.45 |
| $C_4–C_5–C_6$ | 131.1 | 127.9 | 130.7 | 130.5 |
| $CO_{ax}–W–CO_{eq}$ | 90.3 | 90.0 | 90.2 | 92.0 |
| $CO_{ax}–W–CO_{eq}$ | 90.2 | 90.2 | 90.1 | 89.9 |
| $CO_{ax}–W–N$ | 0.0 | 28.85 | 0.0 | 25.3 |
| $NC_4–C_5–C_6$ | 0.0 | 102.24 | 0.0 | 88.3 |

ground state, the low-lying excited states will be generated by excitations from the d orbitals of tungsten to the low-lying $\pi^*_{C=C}$ and $\pi^*_{CO}$ orbitals localized on the pyridine and carbonyl ligands.

The CASSCF/MS-CASPT2 and TD-DFT/B3LYP calculated electronic Franck–Condon transitions of complex **1** are reported in Table 2. The electronic absorption spectrum of complex **1** is essentially composed of MLCT transitions with a high density of states between 18 600 and 30 800 $cm^{-1}$. Two intense absorptions are calculated at 18 620 $cm^{-1}$ (or 537 nm) and 24 190 $cm^{-1}$ (or 413 nm), both corresponding to excitations to the $\pi^*_{C=C}$ orbitals localized on the pyridine group, with significant oscillator strengths of 0.223 and 0.114, respectively. The upper part of the spectrum (beyond 395 nm) is composed of weakly absorbing MLCT states ($5d_W \rightarrow \pi^*_{CO}$).

The transition calculated at 18 620 $cm^{-1}$ (537 nm) can be assigned to the experimental band appearing at 490 nm in benzene and at 522 nm in cyclohexane. Indeed, a value of the oscillator strength equal to 0.25 was determined for the band at 490 nm in benzene (unfortunately **1** has a very low solubility in the latter solvent and a saturated solution of unknown concentration was used for the measurements, making it impossible to determine the oscillator strength of this transition). The second state of **1** calculated at 24 190 $cm^{-1}$ (413 nm) agrees with the experimental spectrum with a band at 406 nm. The upper part of the experimental spectrum between 325–440 nm is characterized by a broad, featureless absorption composed essentially of MLCT ($5d_w \rightarrow \pi^*_{CO}$) states. It is worth noting that the orbital $d_{yz}$ involved in the lowest energy transition in the MS-CASPT2 calculations has a contribution from the $\pi_{C=C}$ orbital as illustrated in Fig. 3.

The interaction between these two orbitals is antibonding, destabilizing the $5d_{yz}$ orbital and promoting electron transfer from this orbital. The agreement between MS-CASPT2 and TD-DFT calculated excited states is qualitatively good and results in the same assignment, namely the presence of MLCT states in the visible domain of energy. However, the transition energies are systematically underestimated by the TD-DFT method for MLCT states corresponding to excitations to $\pi^*_{C=C}$ orbitals. This is due to the difficulty of the DFT approach in describing charge transfers between highly delocalized centers.[24] As a consequence, the energetic order is not the same at the MS-CASPT2 and TD-DFT levels of theory, the latter assigning the three lowest states to excitations to the $\pi^*_{C=C}$ orbitals localized on the pyridine ligand.

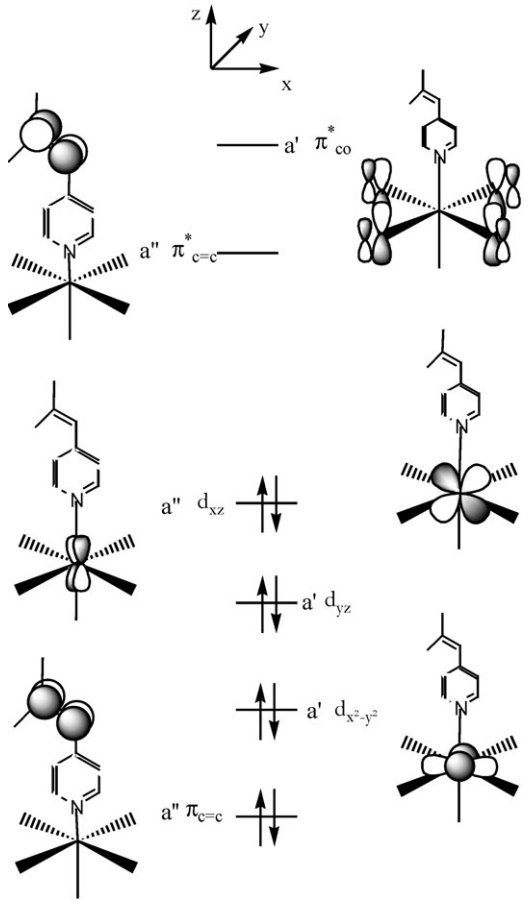


**Fig. 2** Molecular orbital diagram showing the high-lying occupied and low-lying vacant orbitals of complexes **1** and **2**.

**Table 2** CASSCF/MS-CASPT2 and TD-DFT transition energies (in $cm^{-1}$) to the low-lying singlet excited states of complex **1** and associated oscillator strengths (in parenthesis).

| Transition | One-electron excitation in the main configuration | MS-CASPT2 | TD-DFT |
|---|---|---|---|
| $a^1A' \rightarrow b^1A'$ | $5d_{yz} \rightarrow \pi^*_{C=C}$ | **18 620 (0.223)** | 16 580 |
| $a^1A' \rightarrow a^1A''$ | $5d_{xz} \rightarrow \pi^*_{C=C}$ | 20 930 ($< 10^{-4}$) | 15 230 |
| $a^1A' \rightarrow b^1A''$ | $5d_{yz} \rightarrow \pi^*_{CO}$ | **22 710 (0.03)** | 23 960 |
| $a^1A' \rightarrow c^1A'$ | $5d_{xz} \rightarrow \pi^*_{CO}$ | **23 680 (0.012)** | 24 380 |
| $a^1A' \rightarrow c^1A''$ | $5d_{x^2-y^2} \rightarrow \pi^*_{C=C}$ | **24 190 (0.114)** | 18 480 |
| $a^1A' \rightarrow d^1A'$ | $5d_{x^2-y^2} \rightarrow \pi^*_{CO}$ | 25 160 ($< 10^{-4}$) | 25 410 |
| $a^1A' \rightarrow d^1A''$ | $5d_{yz} \rightarrow \pi^*_{CO(eq)}$ | 26 530 ($10^{-3}$) | |
| $a^1A' \rightarrow e^1A'$ | $5d_{xz} \rightarrow \pi^*_{CO(eq)}$ | 27 540 ($10^{-4}$) | |
| $a^1A' \rightarrow e^1A''$ | $5d_{xz} \rightarrow \pi^*_{CO(eq)}$ | 29 880 ($10^{-4}$) | |
| $a^1A' \rightarrow f^1A'$ | $5d_{yz} \rightarrow \pi^*_{CO(eq)}$ | **30 860 (0.04)** | |

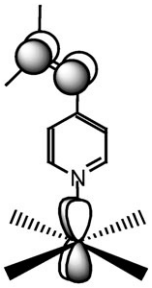

**Fig. 3** Interaction between $5d_{yz}$ (W) and $\pi_{C=C}$ orbitals.

In order to compare the absorption spectra of complexes **1** and **2**, low cost TD-DFT calculations were performed on both complexes. The TD-DFT transition energies of complexes **1** and **2** are reported in Table 3 for comparison.

The Franck–Condon regions of both complexes are similar and the only difference is that transitions toward $\pi_{(C=C)}$ are 600–900 $cm^{-1}$ lower in energy for complex **2**. According to the similar results obtained at the TD-DFT level, it was not necessary to carry out costly CASSCF/MS-CASPT2 calculations for this complex.

In conclusion, the computational study showed that complexes **1** and **2** have two low-lying MLCT excited states corresponding to electron transfer from the metal to the antibonding $\pi_{C=C}$ orbital of the vinyl group in position 4 of the pyridine ring. The three higher excited states are also MLCT states, but here the electron is transferred to the CO ligands. Similarly to complexes of pyridine and 4-cyanopyridine, the d-d excitations are at higher energy and do not appear in the visible region. A negative solvatochromism has been observed for the low energy MLCT band, as described in more details in a previous study.[11]

### Nanosecond laser photolysis of compounds 1 and 2 in toluene and dioxane

Compounds **1** and **2** in toluene and dioxane solutions have been found to be nonfluorescent when excited at wavelengths between 300 and 500 nm. After excitation of both compounds by the 7 ns–532 nm pulse in either toluene or dioxane nitrogen-saturated solutions, a transient absorption spectrum is observed with a positive absorbance change $\Delta A$ from 350 to 850 nm (the limit of our detection setup). This transient absorbance change in both solvents is depicted in Fig. 4 in the case of compound **1**.

It is worth noting that the dip in the measured absorbance change $\Delta A$ observed around 500 nm corresponds approximately to the maximum of absorbance of the ground state: 490 nm in toluene and 460 nm in dioxane for compound **1**. This results from the depopulation of the ground state. In order to obtain the true absorption spectrum of this nanosecond transient (henceforth called **X**), we added to the observed spectrum a fraction of the initial absorbance adjusted so that the dip around 500 nm disappears in the final spectrum. This method has been previously used when ground state and excited state

**Table 3** TD-DFT transition energies (in $cm^{-1}$) to the low-lying singlet excited states of compounds **1** and **2**

| Transition | One-electron excitation in the main configuration | **1** | **2** |
|---|---|---|---|
| $a^1A' \rightarrow a^1A''$ | $5d_{xz} \rightarrow \pi^*_{C=C}$ | 15 230 | 14 320 |
| $a^1A' \rightarrow b^1A'$ | $5d_{yz} \rightarrow \pi^*_{C=C}$ | 16 580 | 15 960 |
| $a^1A' \rightarrow c^1A''$ | $5d_{x^2-y^2} \rightarrow \pi^*_{C=C}$ | 18 480 | 17 530 |
| $a^1A' \rightarrow b^1A''$ | $5d_{yz} \rightarrow \pi^*_{co}$ | 23 960 | 24 000 |
| $a^1A' \rightarrow c^1A'$ | $5d_{xz} \rightarrow \pi^*_{co}$ | 24 380 | 24 410 |
| $a^1A' \rightarrow d^1A'$ | $5d_{x^2-y^2} \rightarrow \pi^*_{co}$ | 25 410 | 25 420 |

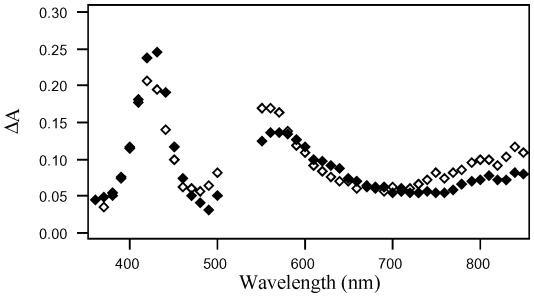


**Fig. 4** End-of-pulse nanosecond absorption spectra of solutions of compound **1**: $1.0 \times 10^{-4}$ M in toluene (◆) and $1.6 \times 10^{-4}$ M in dioxane (◇).

absorption spectra overlap and when the transient extinction coefficient is unknown.[25] It is based on the hypothesis that the final transient spectrum has neither a maximum nor a minimum at the same wavelength as the ground state maximum. This method, which is demonstrated on Fig. 5 for compound **1** in dioxane, although being approximate, allows one to determine an order of magnitude of both extinction coefficients and quantum yields of transient species **X.**

With this method, we have found that transient **X** of compound **1** has an absorption spectrum peaking at 420 nm in both dioxane and toluene, a shoulder around 550 nm and a wide band in the near infrared, with no clear maximum below 850 nm. The extinction coefficient at 420 nm has been determined and is $(1.1 \pm 0.2) \times 10^4$ L $mol^{-1}$ $cm^{-1}$ in both dioxane and toluene, and the quantum yield has been found to be equal to unity. The nanosecond transient spectrum observed after irradiation of compound **2** in toluene is shown in Fig. 6. This spectrum has not been corrected for the negative contribution of the ground state absorption because this absorption has a maximum at 522 nm, which is located in a wavelength domain where transient absorption measurements are experimentally impossible (see Experimental). It is worth noting that as for compound **1** (see Fig. 4) the observed absorption spectrum has a minimum in the wavelength range of the ground state absorption spectrum maximum.

The transient absorption spectrum attributed to species **X** (Fig. 5) is closely similar to the transient excited state absorption spectrum observed after excitation of $W(CO)_5$–pyridine complexes having electron-withdrawing substituents (4-acetylpyridine, 4-benzoylpyridine, 4-cyanopyridine and 4-formylpyridine).[3] This means that the same type of excited state is created for all these compounds. However, in the case of the

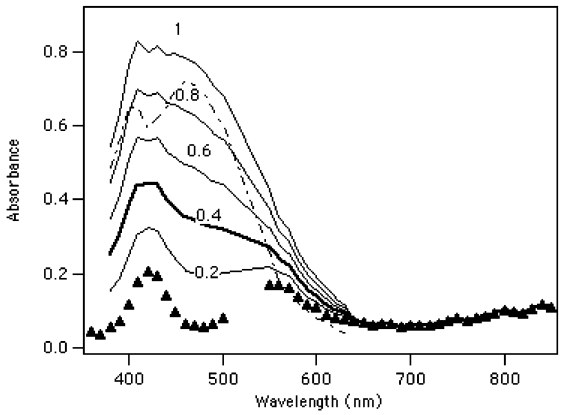


**Fig. 5** Calculated absorption spectrum of transient **X** in dioxane after taking into account the bleaching of the ground state (absorption spectrum of a $10^{-4}$ M solution: dashed line). The calculated spectra (continuous lines) are obtained by summing the observed transient spectrum (triangles) and the ground state absorption spectrum (dashed line), weighted by the coefficient shown on the curves. The curve with the bold line (coefficient 0.4) is attributed to transient **X** (see text).

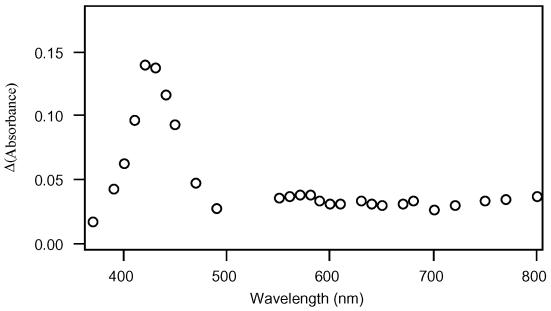


**Fig. 6** Differential absorption spectrum obtained at the end of the nanosecond pulse for compound **2** ($1.25 \times 10^{-4}$ M in toluene).

compounds studied in ref. 3, this excited state, identified as the M → pyridine CT state, is luminescent with a long lifetime (several hundreds of nanoseconds in benzene at room temperature) measured on both the transient absorption and the luminescence decays, but, in contrast, our compounds are not luminescent. This difference will be discussed below.

The decay of transient **X** for deaerated solutions of **1** and **2** in toluene and dioxane was successfully fitted with a first-order kinetics. An example is shown in Fig. 7 for compound **1** in toluene. The decay times ($\tau_X$) of transient **X** are presented in Table 4.

### Picosecond laser photolysis of compounds 1 and 2 in toluene and in dioxane

In order to check whether transient **X** is the primary photoexcited state, we performed laser photolysis of **1** and **2** with a shorter time resolution, using a picosecond laser pulse.

Transient absorption spectra obtained at the end of the 30 ps pulse for compounds **1** and **2** in toluene and dioxane are closely similar to those described above for the nanosecond pulse. As an example, Fig. 8 shows the end-of-pulse excited absorption spectrum of compound **1** in dioxane, which is similar to that shown in Fig. 4. This means that in both cases the observed transient is either the primary excited state, or at least an excited state formed from it in less than 100 ps, with a quantum yield of unity, that is, with no nonradiative pathway to the ground state on the time scale extending from 100 ps to 10 ns (the end of the nanosecond pulse).

## Discussion and conclusions

In comparison with $W(CO)_5$ complexes of pyridine derivatives studied previously, compounds **1** and **2** have a pyridine ligand bearing a longer, conjugated substituent composed of the ethylenic π-bridge with two strongly electron-withdrawing substituents. Theoretical calculations confirm the planarity of this ligand, indicating extensive π-conjugation. Some deformations observed in the crystalline state[11] may be due to crystal packing forces. Theoretical calculations also show that the two lowest excited states of **1** and **2** are the MLCT (W → pyridine*) states. They correspond to transitions of electrons from tungsten $d_{x^2-y^2}$ and $d_{yz}$ orbitals to the antibonding $\pi^*_{C=C}$ orbital of the ethylenic bridge in the pyridine ligand. The energy of the lowest electronic transition calculated for **1** is equal to 2.31 eV (537 nm). In the experimental spectrum, this transition appears at 490 nm in benzene and at 522 nm in cyclohexane (as stated above, it was not possible to determine the oscillator strength of this transition in cyclohexane). On the other hand, for the band at 490 nm in benzene a value of the oscillator strength equal to 0.25 was determined (calculated value 0.223). The energy of the lowest excited state of **1** is considerably lower than the values observed or calculated for $W(CO)_5$ complexes of pyridine derivatives studied up to now [*e.g.*, the energy of the lowest MLCT transition of the previously studied $W(CO)_5$–(4-cyanopyridine) complex was calculated to be at 3.13 eV and observed at 3.25 eV ].

**Table 4** Decay times $\tau_X$ (in ns) of transient **X** for compounds **1** and **2** in toluene and dioxane

| | Dioxane | Toluene |
|---|---|---|
| **1** | 5 ± 1 | 25 ± 1 |
| **2** | 3 ± 1 | 12 ± 2 |

The electronic absorption spectra of the transient species formed upon photolysis of **1** and **2** resemble closely those reported earlier for other $W(CO)_5$–pyridine complexes and assigned to M → pyridine* CT excited states.[3] Due to a strong spin–orbit coupling induced by the tungsten atom, the singlet or triplet nature of these excited states will not be considered here. For compounds **1** and **2**, these states are formed with quantum yields close to 1 after nanosecond excitation and decay directly to the ground states. Their spectra are unchanged when going from 0.1 to 10 ns resolution spectroscopy. Therefore, we can conclude that these transient states are the primary ones formed after visible light excitation and relaxation of the nuclei and the solvent from the initially populated Franck–Condon states, as proposed before for other $W(CO)_5$–pyridine complexes.[3] However, the lifetimes of the excited states of **1** and **2** are about 10 times shorter than those observed previously for similar complexes. For example, the excited state of the 4-cyanopyridine complex has a lifetime of 219 ns in benzene at 20 °C,[3] compared to a lifetime of 25 ns for compound **1** in toluene at the same temperature. Furthermore, the transient absorption spectra following laser flash photolysis of 4-cyanopyridine and related complexes display a residual permanent absorption indicating that a chemical reaction occurs in the irradiated system. This reaction is presumably the formation of $W(CO)_5$–solvent species. The residual permanent absorption has not been observed in transient spectra measured in experiments with **1** and **2** at any monitoring wavelength. This means that dissociation of the pyridine ligand is not an important relaxation pathway for the excited states of these complexes. Otherwise, when compared to other $W(CO)_5$–pyridine complexes, **1** and **2** are rather photostable compounds. No solution decomposition of these compounds was

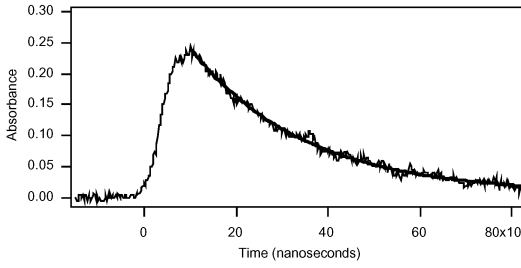


**Fig. 7** Decay of transient absorbance at 420 nm following nanosecond laser photolysis of compound **1** ($5.5 \times 10^{-5}$ M in toluene). The calculated curve corresponds to a fit with an exponential function (decay time: 24.8 ns).

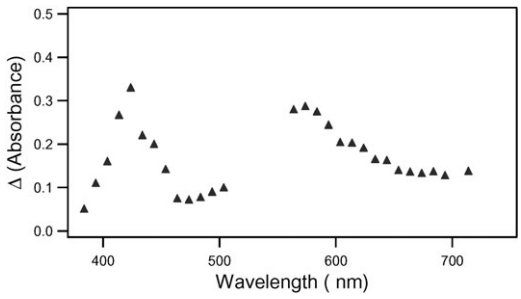


**Fig. 8** Differential absorption spectrum obtained at the end of the picosecond pulse for compound **1** ($4.1 \times 10^{-4}$ M in dioxane).

observed, even after several hundreds of laser pulses. This corroborates a generally accepted statement that ligand substitution reactions in $W(CO)_5$–pyridine originate from the LF (or M → CO* CT, according to recent theoretical calculations[9]) transitions. Although for the 4-cyanopyridine the M → pyridine* CT state is the lowest excited state, the dissociative state can be populated thermally and leads to ligand substitution in low quantum yields. The extremely low energy of M → pyridine* CT states in complexes **1** and **2**, together with their short lifetimes, make thermal population of dissociative states highly improbable, thus explaining the photostability of these complexes. So our results corroborate that the low energy transitions are MLCT ones.

Another striking difference between **1** and **2** and their 4-cyanopyridine analog is that the latter exhibits luminescence from the M → pyridine* CT state, whereas **1** and **2** are not photoemissive. This may result from a very efficient nonradiative deactivation of the M → pyridine* CT state for **1** and **2**. In fact, it has been found for the emissive complexes that the luminescence quantum yields decrease with the lifetimes of the M → pyridine* CT states.[3] Consequently, for lifetimes as short as $\sim 10^{-8}$ s, the intensity of luminescence may be below the detection limit of our time resolved nanosecond laser photolysis setup. However, with an oscillator strength of 0.25 for compound **1** in benzene, one can estimate the radiative lifetime to be as short as 10 ns. As no fluorescence is observed—which means a fluorescence quantum yield lower than $10^{-4}$—a nonradiative rate constant higher than $10^{12}$ $s^{-1}$ can be inferred. Such a very fast deactivation process is not consistent with the observed lifetimes of transient **X** (several nanoseconds). As a result, we formulate the hypothesis that transient **X** is not the primary MLCT excited state, but a transient intermediate issued from it on a very short time scale (shorter than 100 ps, our fastest time resolution). The very fast relaxation process may be a change in geometry of the substituted pyridine ligand following the charge transfer, as for example a twisting around the double bond. This excited state with a distorted geometry of the nuclei would then relax on a nanosecond time scale to the ground state. Femtosecond laser experiments would be needed to clarify this process.

Finally, the lifetimes of the excited states of **1** and **2** follow the previously observed dependence on the solvent polarity: more polar solvents, shorter lifetimes. This can be considered as a consequence of the energy gap law,[26] that is, the smaller the energy gap between the excited and the ground states, the faster the nonradiative pathways leading to deactivation of the excited state.



## References


1 M. S. Wrighton, H. B. Abrahamson and D. L. Morse, *J. Am. Chem. Soc.*, 1976, **98**, 4105.
2 R. M. Dahlgren and J. I. Zink, *Inorg. Chem.*, 1977, **16**, 3154.
3 A. J. Lees and A. W. Adamson, *J. Am. Chem. Soc.*, 1982, **104**, 3804.
4 C. Moralejo, C. H. Langford and D. K. Sharma, *Inorg. Chem.*, 1989, **28**, 2205.
5 S. Wieland, R. van Eldik, D. R. Crane and P. C. Fort, *Inorg. Chem.*, 1989, **28**, 3663.
6 K. A. Rawlins, A. J. Lees and A. W. Adamson, *Inorg. Chem.*, 1990, **29**, 3866.
7 P. Glyn, F. P. A. Johnson, M. W. George, A. J. Lees and J. J. Turner, *Inorg. Chem.*, 1991, **30**, 3543.
8 F. P. Johnson, M. W. George and J. J. Turner, *Inorg. Chem.*, 1993, **32**, 4226.
9 S. Záliš, A. Vlček Jr and C. Daniel, *Collect. Czech. Chem. Commun.*, 2003, **68**, 89.
10 S. Di Bella, *Chem. Soc. Rev.*, 2001, **30**, 355.
11 A. Hameed, A. Rybarczyk-Pirek and J. Zakrzewski, *J. Organomet. Chem.*, 2002, **656**, 102.
12 D. Andrae, U. Haeussermann, M. Dolg, H. Stoll and H. Preuss, *Theor. Chim. Acta*, 1990, **77**, 123.
13 A. Bergner, M. Dolg, W. Kuechle, H. Stoll and H. Preuss, *Mol. Phys.*, 1993, **80**, 1431.
14 S. Huzinaga, *J. Chem. Phys.*, 1965, **42**, 1293.
15 I. Cote-Bruand, unpublished data.
16 E. Runge and E. K. U. Gross, *Phys. Rev. Lett.*, 1984, **52**, 997.
17 B. O. Ross, P. R. Taylor and P. E. M. Siegbahn, *Chem. Phys.*, 1980, **48**, 157.
18 J. Finley, P.-A. Malmqvist, B. O. Roos and L. Serrano-Andrés, *Chem. Phys. Lett.*, 1998, **288**, 299.
19 M. J. Frisch, G. W. Trucks, H. B. Schlegel, G. E. Scuseria, M. A. Robb, J. R. Cheeseman, V. G. Zakrzewski, J. A. Montgomery, Jr., R. E. Stratmann, J. C. Burant, S. Dapprich, J. M. Millam, A. D. Daniels, K. N. Kudin, M. C. Strain, O. Farkas, J. Tomasi, V. Barone, M. Cossi, R. Cammi, B. Mennucci, C. Pomelli, C. Adamo, S. Clifford, J. Ochterski, G. A. Petersson, P. Y. Ayala, Q. Cui, K. Morokuma, P. Salvador, J. J. Dannenberg, D. K. Malick, A. D. Rabuck, K. Raghavachari, J. B. Foresman, J. Cioslowski, J. V. Ortiz, A. G. Baboul, B. B. Stefanov, G. Liu, A. Liashenko, P. Piskorz, I. Komaromi, R. Gomperts, R. L. Martin, D. J. Fox, T. Keith, M. A. Al-Laham, C. Y. Peng, A. Nanayakkara, M. Challacombe, P. M. W. Gill, B. G. Johnson, W. Chen, M. W. Wong, J. L. Andres, C. Gonzalez, M. Head-Gordon, E. S. Replogle and J. A. Pople, *GAUSSIAN 98 (Revision A.11)*, Gaussian, Inc., Pittsburgh, PA, 2001.
20 K. Andersson, M. Barysz, A. Bernhardsson, M. R. A. Blomberg, D. L. Cooper, M. P. Fülscher, C. de Graaf, B. A. Hess, G. Karlström, R. Lindh, P.-Å. Malmqvist, T. Nakajima, P. Neogrády, J. Olsen, B. O. Roos, B. Schimmelpfennig, M. Schütz, L. Seijo, L. Serrano-Andrés, P. E. M. Siegbahn, J. Stålring, T. Thorsteinsson, V. Veryazov and P.-O. Widmark, *MOLCAS, Version 5.0*, Lund University, Sweden, 2000.
21 P. Feneyrou, F. Soyer, P. Le Barny, E. Ishow, M. Sliwa and J. A. Delaire, *Photochem. Photobiol. Sci.*, 2003, **2**, 195.
22 I. Texier, J. A. Delaire and C. Giannotti, *Phys. Chem. Chem. Phys.*, 2000, **2**, 1205.
23 M. Sumitani and K. Yoshihara, *Bull. Chem. Soc. Jpn*, 1982, **55**, 85.
24 M. E. Cassida, F. Guttierez, J. Guan, F.-X. Gadea, D. R. Salahub and J.-P. Daudey, *J. Chem. Phys.*, 2000, **113**, 7062.
25 Y. H. Meyer and P. Plaza, *Chem. Phys.*, 1995, **200**, 235.
26 N. J. Turro, *Modern Molecular Photochemistry*, The Benjamin/Cummings Publishing Co., Inc., Menlo Park, CA, USA, 1978, p. 183.